Desalination and Water Treatment
www.deswater.com

doi: 10.1080/19443994.2015.1106344

57 (2016) 20049–20057
September

Taylor & Francis
Taylor & Francis Group

Reduced graphene oxide modified luffa sponge as a biocomposite adsorbent for effective removal of cationic dyes from aqueous solution

Shengfang Li[a,b,*], Min Tao[b], Yongdi Xie[a]

[a]*School of Chemistry and Chemical Engineering, Hubei Polytechnic University, Huangshi 435003, P.R. China, Tel./Fax: +86 714 6367957; email: lishengf_@163.com (S. Li)*
[b]*Hubei Key Laboratory of Mine Environmental Pollution Control and Remediation, Hubei Polytechnic University, Huangshi 435003, P.R. China*

Received 9 February 2015; Accepted 2 October 2015

ABSTRACT

Natural luffa sponge (LS) was modified by reduced graphene oxide (RGO) by one-step hydrothermal treatment of LF in GO suspensions with the assistance of ascorbic acid. The obtained RGO-modified LF sponge (RGL) was studied by X-ray diffraction, Fourier-transform infrared, and scanning electron microscope (SEM). The results suggested that a biocomposite with about 500 nm pore diameter, which can effectively enhance the adsorption capacity properties of LS. The batch adsorption studies demonstrated that the adsorption of RGL toward cationic dyes highly depended on the initial pH of solution, RGO content and initial concentration of dyes. The incorporation of RGO can increase the adsorption capacities of LS significantly. The value of the uptake of cationic dyes at equilibration time (q_e), for basic magenta (BM), increased from 32.56 to 88.32 mg/g, while for methylene blue (MB), increased from 31.65 to 63.32 mg/g, when the content of RGO increased from 0 to 0.4 wt%. It was found that the adsorption kinetics data fitted with pseudo-second-order model and adsorption isotherm followed the Langmuir model well. The electrostatic interaction played a major role in the adsorption process.

Keywords: Reduced graphene oxide; Luffa sponge; Cationic dye; Kinetics; Isotherm

1. Introduction

Nowadays, dye wastewater in textile industries has become a great environmental problem. These dyes in wastewater are very toxic and can affect human health seriously when they are discharged into water [1]. In addition, many dyes are difficult to biodegrade and cannot be easily removed by conventional wastewater treatment processes due to their complex aromatic molecular structure and synthetic origins [2,3]. Therefore, how to remove dyes effectively from aqueous solution is still a serious problem. In the past years, many methods, such as adsorption, chemical precipitation, photodegradation, ion exchange, osmosis, and ultra filtration membrane separation, etc. have been developed for the removal of dyes from aqueous solution. Among these technologies, adsorption has attracted much attention due to its simplicity of design, economic feasibility, high efficiency, and ease of operation [4–6].

Various adsorbents have been used for the removal of dyes from aqueous solution. Many natural

*Corresponding author.

adsorbents, i.e. hazelnut shell, seashell, bottom ash, eggshell and hen feather and luffa sponge (LS), are being paid more attention because that they are abundant and low cost [7–17]. LS is a typical natural adsorbent which is consisted of cellulose and lignin. This natural sponge possesses continuous hollow microchannels that form vascular bundles and yield a multimodal hierarchical pore system. Recently, LS have been applied as adsorbents for dyes removal from aqueous solution. However, the adsorption capacity of pure natural LS is still limited [18–20].

Graphene is a new carbon material with a two-dimensional structure and outstanding properties. The ultra-large specific surface area (theoretically 2,630 $m^2 g^{-1}$) and flat structure make graphene an excellent adsorbent for wastewater treatment [21–25]. Different GO and reduced graphene oxide (RGO) modified composite have been synthesized and applied in wastewater treatment [26–32]. Herein, we present a convenient, effective method to modify natural LS with RGO. A highly porous RGO modified LS (RGL) was obtained by one-step hydrothermal treatment of LS in GO suspensions with the assistance of ascorbic acid. The as-prepared porous RGL showed high adsorption capacity for the removal of BM and MB from aqueous solutions. The adsorption behavior and influencing factors such as the initial pH of solution, RGO content, and initial concentration of dyes were investigated in details.

2. Experimental

2.1. Chemicals and materials

The graphite was purchased from Huadong Graphite Co. China. Ascorbic acid, BM [molecular formula, $C_{20}H_{20}ClN_3$; molecular weight, 337.85] and MB [molecular formula, $C_{16}H_{18}N_3SCl$; molecular weight, 319.86] were purchased from Tianjin Chemical Reagent Co. China. LS were obtained from a local shop, Huangshi, China. It was washed with acetone in an ultrasonic bath at room temperature for 10 min and then rinsed with water and dried at 60°C. After drying, LS was treated in a sodium hydroxide solution (NaOH, 0.1 M) at 60°C for 2 h. This treatment was repeated 3 times to activate the cellulose fiber of LS. After the treatment, LS was cut to form a cylinder with diameter of 3 cm and height of 1 cm and was stored for use.

2.2. Preparation of GO

GO was prepared according to modified Hummers′ method [33]. The product was dialyzed by deionized water for one week. Finally, the product was centrifuged at 10,000 rpm for 2 h and dried at 333 K.

2.3. Preparation of RGL

As shown in Fig. 1, the RGL was prepared by hydrothermal treatment of LS in GO suspensions with the assistance of ascorbic acid. Firstly, a stoichiometric quantity of ascorbic acid was added into GO aqueous dispersion. LS was placed in above mixture solution and then sealed in a 100 mL Teflon-lined stainless steel autoclave and maintained at 90°C for 8 h. After that, the RGL was formed. It was dipped into distill water for 24 h to remove the residual ascorbic acid. Finally, vacuum freezedrying was used to remove water and a black porous product can be obtained. According to the calculation of the dry weight of LS before and after hydrothermal reaction treatment, the content of RGO in RGL can be measured.

2.4. Characterization

The morphologies of samples were investigated using a scanning electron microscope (SEM) (JSM-5610LV) and a transmission electron microscope (TEM, JEM-2100) operated at 200 kV. The phase structure was examined by X-ray diffraction (XRD) using a Philips PW1140/90 diffractometer with Cu Kα radiation (25 mA and 40 kV) at a scan rate of 2° min^{-1} with a step size of 0.02°. Fourier-transform infrared (FTIR) spectra were recorded on a Perkin Elmer FTIR spectrometer by using the KBr wafer technique.

2.5. Batch adsorption studies

Batch adsorption experiments were carried out at 25°C, in magnetically stirred (160 rpm) cylindrical glass vessels in batch conditions [34–36]. The stoichiometric quantity of RGL was added in 50 mL of 60–120 mg/L dye solution. The value of the uptake of cationic dyes at equilibration time (q_e) was analyzed by a using a 1650PC UV–visible spectrophotometer according to the following equation:

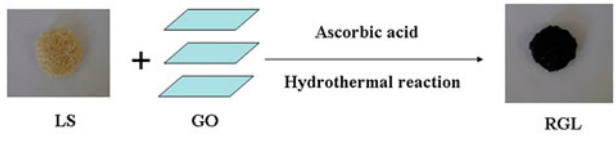

Fig. 1. Schematic illustration of preparation of RGL.

$$q_e = \frac{(C_0 - C_e)V}{m} \quad (1)$$

where V is the solution volume (mL), m is the weight of dried adsorbent (g), C_0 and C_e is the dye concentration at initial and equilibrium time (mg/L), respectively. All the experiments were conducted in triplicate, and the average results are reported in this paper.

2.6. Desorption and reusability studies

Desorption studies were performed with a mixture solution of HCl and ethanol. RGL adsorbed with dye was agitated in the mixture solution for 1 h. The amount of the dye released into the mixture solution was determined by spectrophotometer. After the completed desorption, RGL was dried by vacuum drying for repeated use.

3. Results and discussion

3.1. Preparation and characterization of RGL

GO were prepared by the oxidation of pristine graphite via a modified Hummer's method. After the oxidation and ultrasonic treatment of pristine graphite, the resulting GO can form a stable dispersion in water. Fig. 2(a) shows the XRD patterns for GO and pristine graphite. It is clear that a diffraction peak of GO appeared at 9.80°, while the diffraction peak of graphite at 26.60° disappeared. This indicated that GO had been successfully synthesized in our experiment [37–39].

The XRD patterns of GO, LS, and RGL were further compared (Fig. 2(b)). As stated earlier, the characteristic diffraction peak of GO appeared at 9.80°, while the characteristic diffraction peaks of pure LS were observed at 15.76° and 22.24°, respectively. However, for RGL the diffraction peaks of GO at 9.8° disappeared, and the characteristic diffraction peaks were found at 15.76°, 22.24°, and 26.21°, respectively. The new diffraction peak at 26.21° was assigned to the characteristic diffraction peak of RGO [40]. This inferred that GO had been reduced to RGO and grafted on the LS. Fig. 3 shows the FTIR spectra of RGO, LS and RGL, respectively. On the FTIR spectrum of RGO, the bands at 1,637 and 1,057 cm^{-1} are attributed to the stretches of aromatic C=C bond and C−O stretch vibrations. Furthermore, compared with pure LS [41,42], an additional peak at 1,731 cm^{-1} corresponding to C=O stretching vibration in RGL was observed. This indicated the reaction between –COOH of RGO and –OH of LS had occurred. In addition, for the FTIR spectra of RGO, LS and RGL, the peaks at 3,423 cm^{-1} are assigned to –OH in carboxyl groups, which will play an important role in the adsorption of cationic dyes [43].

Fig. 4 shows the digital camera and SEM images of RGL. Obviously, RGL is a black porous composite. From the SEM photograph of the RGL, many pores with diameter of about 500 nm can be observed on the wall of sponge. The thin nanosheets of RGO were inserted between the walls of sponge. This unique structure can effectively enhance the adsorption capacity properties of RGL.

3.2. Effect of initial pH of solution on adsorption

Fig. 5 shows the q_e of RGL, with 0.4 wt% GO, for BM and MB in aqueous solutions with different pH values. It can be clearly seen that, for BM and MB, the adsorption ability of RGL was greatly influenced by the solution. The value of q_e for BM and MB was dramatically increased from 33.0 to 75.1 mg/g for BM and 19.2 to 56.3 mg/g for MB, as the pH value of

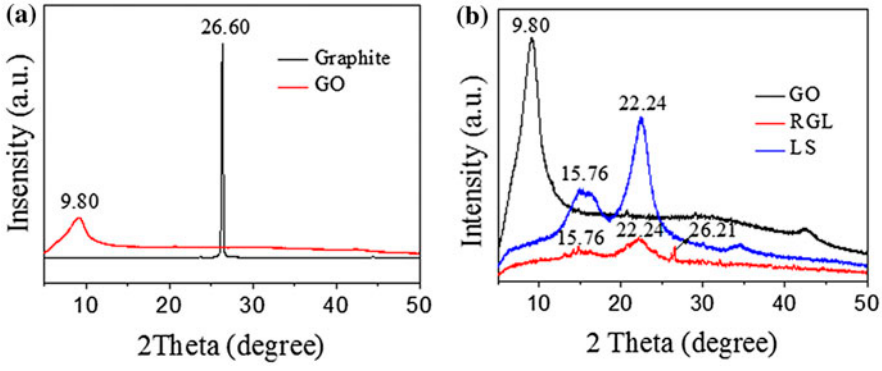

Fig. 2. XRD patterns of GO and graphite (a); GO, LS, and RGL (b).

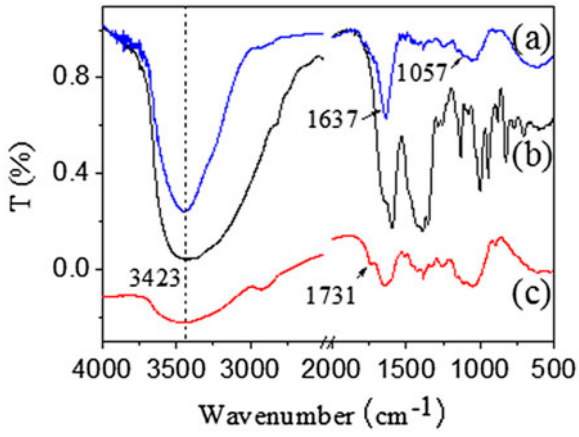

Fig. 3. FTIR spectra of RGO (a), LS (b), and RGL (c).

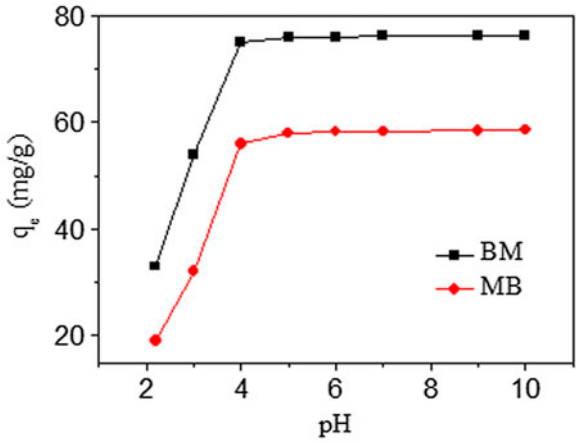

Fig. 5. The effect of initial pH of solution on adsorption (0.4 wt% RGO; initial concentration of BM and MB: 100 mg/L).

solution changed from 2.2 to 4.0. At low pH, the carboxyl groups of the LS became protonated, and electrostatic repulsions between the cationic dyes (BM and MB) and the H_3O^+ ions may prevent the adsorption of the cationic dyes (BM and MB) onto RGL, resulting in a low adsorption capacity of RGL toward BM and MB. As the pH value of solution increased, when pH > 4.0, more carboxyl groups became deprotonated and the electrostatic force of attraction between RGL and cationic dyes molecules increased the uptakes of BM and MB [43]. Since RGL show a high adsorption capability for cationic dyes when pH > 4.0. So, pH > 4.0 was chosen for subsequent adsorption experiments.

3.3. Effect of content of RGO on adsorption

Fig. 6 shows the adsorption capacities of RGL toward BM and MB with different RGO contents. For both BM and MB, the values of q_e were markedly

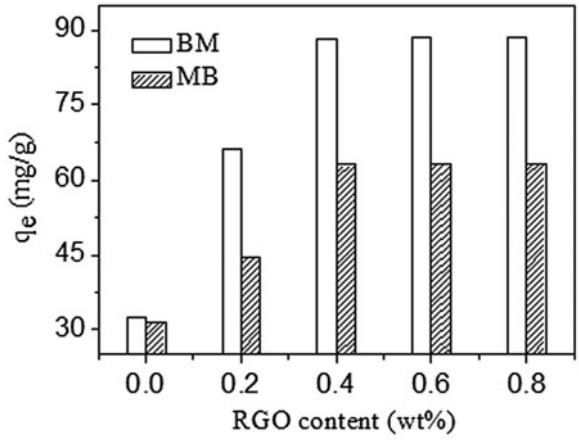

Fig. 6. The effect of content of RGO on adsorption (pH value of the solution: 7.0; initial concentration of BM and MB: 120 mg/L).

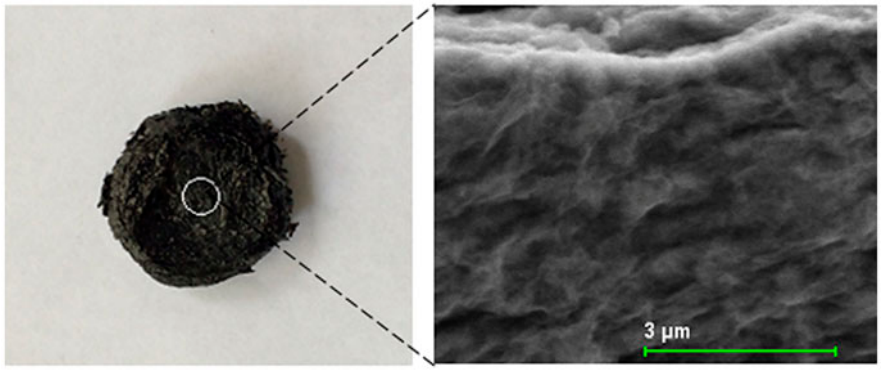

Fig. 4. Digital camera and SEM images of RGL.

increased when the content of RGO increased from 0.0 to 0.4 wt% (for BM, increased from 32.56 to 88.32 mg/g, while for MB, increased from 31.65 to 63.32 mg/g). When the content of RGO > 0.4 wt%, the values of q_e of RGL did not increased and almost kept a constant. This indicated that the incorporation of RGO can indeed increase the adsorption capacities of RGL toward cationic dyes. This is mainly attributed to the adsorption of RGO in the RGL through strong π-π stacking and anion–cation interactions, as well as the large specific surface area and mesoporous structure of the materials [44–46].

3.4. Effect of initial concentration of dyes on adsorption

The effect of dye initial concentration on adsorption of BM and MB onto RGL was investigated (Fig. 7). When the dye concentration was increased from 60 to 120 mg/L, the values of q_e gradually increased and reached a maximum (for BM: 86.98 mg/g; for MB: 63.31 mg/g), which was the saturated adsorption amount. It can be explained that a higher concentration of cationic dyes, more cationic dyes molecules interacted with RGL, leading to an increase in adsorption of RGL.

3.5. Adsorption kinetics

Fig. 8 shows the kinetics of adsorption of BM and MB onto RGL in different initial dye solutions. For both dyes, the adsorption increased with the contact time. In order to have an insight into the mechanism of adsorption process, kinetics models including the pseudo-first-order and pseudo-second-order models

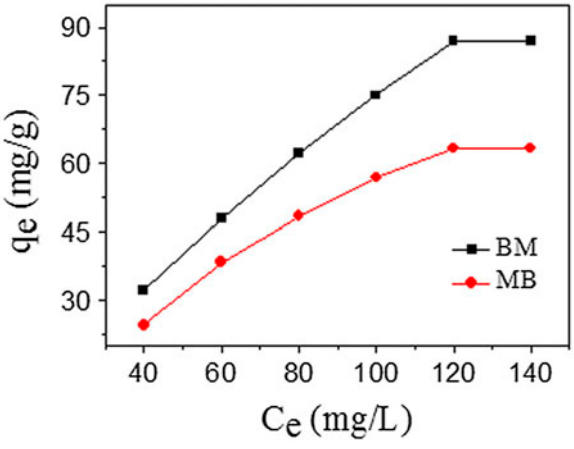

Fig. 7. The effect of initial concentration of BM and MB on adsorption (0.4 wt% RGO; pH value of the solution: 7.0).

were used to analyze the experiment data [47,48]. They are given as Eqs. (2) and (3), respectively:

$$\ln(q_e - q_t) = \ln q_e - k_1 t \tag{2}$$

$$\frac{t}{q_t} = \frac{1}{k_2 q_e^2} + \frac{t}{q_e} \tag{3}$$

where q_e is equilibrium adsorption amount (mg/g), and k_1 is the pseudo-first-order rate constant (min). q_t is the amount of adsorption dye (mg/g) at time (min) and k_2 is the pseudo-second-order rate constant (g/mg/min). The constants were determined experimentally by plotting $\ln(q_e - q_t)$ vs. time and t/q_t vs. time. The results are listed in Table 2.

As can be seen in Fig. 8, during the first 20 min, all samples exhibited fast adsorption rate and reached equilibrium within 150 min. From Table 1, it can be found that, for BM and MB, the correlation coefficients (R^2) of Pseudo-second-order kinetics (0.956, 0.976, 0.990, 0.960, 0.988, 0.981, 0.951, and 0.913, respectively) were higher than that of Pseudo-first-order kinetics (0.996, 0.997, 0.998, 0.999, 0.993, 0.999, 0.995, and 0.994, respectively). These confirmed that the adsorption of cationic dyes on RGL followed pseudo-second-order kinetic model well [49].

3.6. Adsorption isotherms

Langmuir and Freundlich equations were employed to study the adsorption isotherms of BM and MB, respectively. The Langmuir isotherm considers the adsorbent surface as homogeneous with identical sites in terms of energy. Langmuir isotherm model [50,51] is given by the following equation:

$$\frac{C_e}{q_e} = \frac{1}{Q_0 b} + \frac{C_e}{Q_0} \tag{4}$$

where q_e is equilibrium adsorption amount and C_e (mg/L) is the equilibrium concentration of dyes, and b is a constant of adsorption equilibrium (L/mg), and Q_0 is the saturated monolayer adsorption capacity (mg/g). $R_L = 1/(1 + bC_0)$, the value of R_L indicates the type of the isotherm to be either unfavorable ($R_L > 1$), linear ($R_L = 1$), favorable ($0 < R_L < 1$), or irreversible ($R_L = 0$).

The Freundlich model [52] based on adsorption on a heterogeneous surface is given by the following equation:

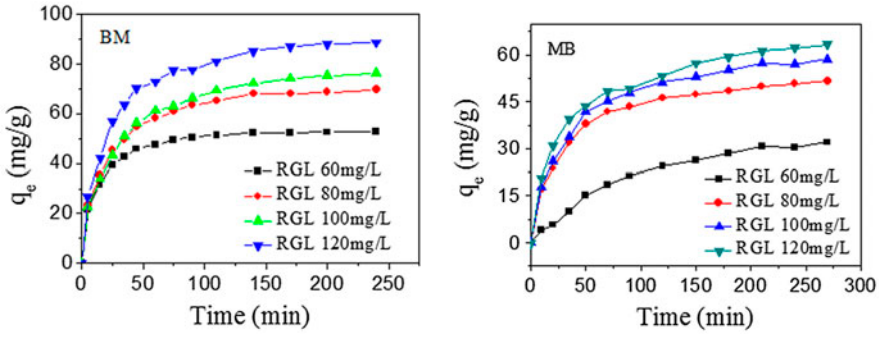

Fig. 8. Kinetics of adsorption of BM and MB onto RGL in different initial dye solutions (0.4 wt% RGO; pH value of the solution: 7.0; 60, 80, 100, and 120 mg/L).

Table 1
Kinetic parameters for adsorption of BM and MB onto RGL

		Pseudo-first-order kinetics			Pseudo-second-order kinetics		
Dye	C_0 (mg/L)	q_e (mg/g)	k_1 (min)	R^2	q_e (mg/g)	k_2 (g/mg/min)	R^2
BM	60	52.48	0.0387	0.956	55.25	0.00007	0.996
	80	68.65	0.0269	0.976	74.63	0.00009	0.997
	100	75.41	0.0212	0.990	83.33	0.00010	0.998
	120	88.30	0.0242	0.960	95.24	0.00004	0.999
MB	60	30.76	0.0157	0.988	11.10	0.00170	0.993
	80	51.61	0.0145	0.981	55.87	0.00017	0.999
	100	57.85	0.0175	0.951	64.52	0.00016	0.995
	120	64.31	0.0325	0.913	66.25	0.00014	0.994

$$\ln q_e = \ln K_F + \frac{1}{n} \ln C_e \quad (5)$$

where K_F and n are Freundlich constants, which represent adsorption capacity and adsorption intensity, respectively.

The Langmuir and Freundlich isotherms obtained from the equilibrium adsorption data in our experiment are shown graphically in Fig. 9 and the isotherm parameters are listed in Table 2. As shown in Fig. 9, all the plots showed a straight line, indicating the adsorption of BM and MB on RGL followed the two isotherms. Comparing the coefficient (R^2) for three isotherms, it was found that the Langmuir isotherm fitted more precisely ($R^2 = 0.997$ and 0.987, respectively.) than Freundlich isotherm ($R^2 = 0.915$ and 0.935, respectively.) Langmuir-type adsorption isotherm was suitable for equilibrium studies indicating the formation of monolayer coverage of BM and MB on the surface of RGL. Moreover, the values of R_L were in the range between 0 and 1 (0.70 and 0.25) and $n > 1$ (4.10 and 5.56), suggesting favorable adsorption of BM and MB onto RGL.

3.7. Thermodynamics studies

The thermodynamic parameters for the adsorption included Gibbs energy (ΔG), enthalpy (ΔH), and entropy (ΔS). These thermodynamic parameters can be calculated according to the following equations:

$$\Delta G = -RT \ln K_d \quad (6)$$

$$K_d = q_e/C_e \quad (7)$$

$$\Delta G = \Delta H - T\Delta S \quad (8)$$

where T is the absolute temperature (K). R is gas constant (J/mol/K), K_d (L/g) is the equilibrium constant. C_e is the dye concentration at equilibrium time. q_e is the equilibrated amount of cationic dyes adsorbed on RGL. According above equations, the following equation can be obtained:

$$\ln K_d = \frac{\Delta S}{R} - \frac{\Delta H}{RT} \quad (9)$$

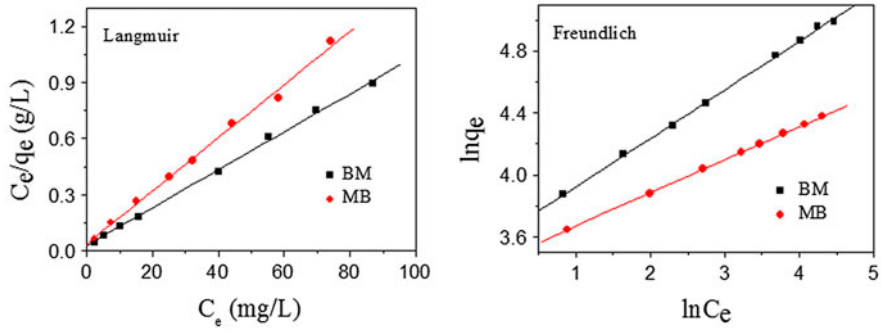

Fig. 9. Langmuir and Freundlich isotherms for the adsorption of BM and MB onto RGL.

Table 2
Langmuir and Freundlich isotherm parameters for the adsorption of BM and MB onto RGL

	Langmuir			Freundlich		
Dye	Q_0 (mg/g)	R_L (L/mg)	R^2	K_F	n	R^2
BM	90.91	0.70	0.997	46.43	4.10	0.915
MB	47.39	0.25	0.987	39.12	5.56	0.935

The values of ΔH and ΔS can be calculated from the slope and the intercept of the plot of $\ln K_d$ vs. $1/T$. The calculated thermodynamic parameters for the adsorption of BM and MB on RGL are given in Table 3. The negative value of ΔG indicated the adsorption reaction was spontaneous.

3.8. Desorption studies

Desorption studies are helpful to explore the possibility of recycling of RGL. Desorption studies were carried out using a mixture of HCl solution (pH 1) and ethanol. Consecutive adsorption–desorption cycles were repeated three times by using the same sorbents. It was found that RGL could be recycled efficiently using the mixture of HCl solution (pH 1) and ethanol.

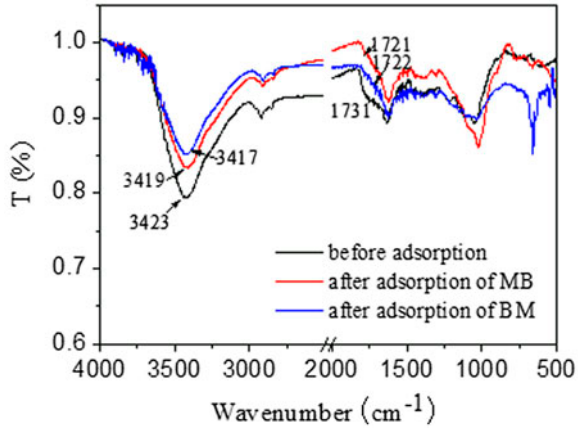

Fig. 10. FTIR spectra of RGL before and after adsorption of BM and MB, respectively.

The efficiency of cationic dyes removal was 86% for BM and 89% for MB after three cycles; this showed that RGL could be reusable.

3.9. Adsorption mechanism

In order to understand the adsorption mechanism of RGL for cationic dyes, the FTIR spectra of RGL

Table 3
Thermodynamic parameters for the adsorption of BM and MB onto RGL at different temperature

Dye	T (K)	ΔG (kJ/mol)	ΔS (J/mol/K)	ΔH (kJ/mol)	R^2
BM	298	−12.31	13.2	12.8	0.997
	303	−12.45			
	308	−12.56			
	312	−12.68			
MB	298	−2.94	8.2	6.6	0.996
	303	−3.12			
	308	−3.86			
	312	−3.54			

before and after adsorption of BM and MB are invested in details. As seen in Fig. 10, the peaks of the stretch vibration of hydroxyl groups and that of C=O stretch vibration of carboxylic groups were shifted from 3,423 and 1,731 cm^{-1} to 3,417 (or 3,419) cm^{-1} and 1,721 (or 1,722) cm^{-1}, respectively. This was attributed to the electrostatic interaction between the carbonyl and hydroxyl groups on the RGL and the cationic dyes molecules. All the shift of absorption bands can illustrate that electrostatic interaction played a major role in the adsorption process.

4. Conclusions

In summary, we have developed a simple hydrothermal treatment method to prepared porous RGL as a biocomposite adsorbent for the effective removal of BM and MB from aqueous solution. The structure of RGL can be adjusted by changing the content of GO. When 0.4 wt% RGO was incorporated into LS, the value of the uptake of cationic dyes at equilibration time (q_e), for BM, increased from 32.56 to 88.32 mg/g, while for MB, increased from 31.65 to 63.32 mg/g. It could be presumed electrostatic interaction involved in the adsorption mechanism. The adsorption kinetics of BM and MB onto RGL followed the pseudo-second-order model and adsorption isotherm fitted Langmuir model well. Desorption experiments showed that RGL could be easily regenerated using a mixture of HCl solution and ethanol. RGL exhibited high adsorption capacities and efficiency for cationic dyes, giving rise to a new generation of green biocomposite adsorbents.

Acknowledgements

The project sponsored by the Scientific Research Foundation for the Returned Overseas Chinese Scholars, State Education Ministry, Hubei provincial Science & Technology Department (2013CFB040), Hubei Polytechnic University (13xjz01A and 2012101), China.

References

[1] A.K. Verma, R.R. Dash, P. Bhunia, A review on chemical coagulation/flocculation technologies for removal of colour from textile wastewaters, J. Environ. Manage. 93 (2012) 154–168.
[2] S. Li, X. Liu, T. Zou, W. Xiao, Removal of cationic dye from aqueous solution by macroporous hydrophobically modified poly(acrylicacid-acrylamide) hydrogel with enhanced swelling and adsorption properties, CLEAN—Soil Air Water 38 (2010) 378–386.
[3] S. Li, S. Yan, J. Yu, Removal of cationic dyes from aqueous solution by hydrophobically modified poly (acrylic acid) Hydrogels, Polym.-Plast. Technol. Eng. 50 (2011) 783–790.
[4] S. Li, Removal of crystal violet from aqueous solution by sorption into semi-interpenetrated networks hydrogels constituted of poly(acrylic acid-acrylamide-methacrylate) and amylose, Bioresour. Technol. 101 (2010) 2197–2202.
[5] V.K. Gupta, Suhas, Application of low-cost adsorbent for dye removal—A review, J. Environ. Manage. 90 (2009) 2313–2342.
[6] G. Sreelatha, S. Kushwaha, V.J. Rao, P. Padmaja, Kinetics and equilibrium studies of adsorption of anionic dyes using acid-treated palm shell, Ind. Eng. Chem. Res. 49 (2010) 8106–8113.
[7] A. Mittal, V. Thakur, J. Mittal, H. Vardhan, Process development for the removal of hazardous anionic azo dye Congo red from wastewater by using hen feather as potential adsorbent, Desalin. Water Treat. 52 (2014) 227–237.
[8] R. Ahmad, P.K. Mondal, Application of acid treated almond peel for removal and recovery of brilliant green from industrial wastewater by column operation, Sep. Sci. Technol. 44 (2009) 1638–1655.
[9] R. Ahmad, Studies on adsorption of crystal violet dye from aqueous solution onto coniferous pinus bark powder (CPBP), J. Hazard. Mater. 171 (2009) 767–773.
[10] P.K. Mondal, R. Ahmad, Application of acid treated water nut activated carbon for the removal of malachite green from industrial waste water by column operation, J. Environ. Res. Dev. 3 (2009) 807–816.
[11] R. Ahmad, P.K. Mondal, Application of modified water nut carbon as a sorbent in congo red and malachite green dye contaminated wastewater remediation, Sep. Sci. Technol. 45 (2010) 394–403.
[12] R. Ahmad, R. Kumar, Adsorption studies of hazardous malachite green onto treated ginger waste, J. Environ. Manage. 91 (2010) 1032–1038.
[13] R. Ahmad, R. Kumar, Kinetic and thermodynamic studies of brilliant green adsorption onto carbon/iron oxide nanocomposite, J. Korean Chem. Soc. 54 (2010) 125–130.
[14] R. Ahmad, R. Kumar, Conducting polyaniline/iron oxide composite: A novel adsorbent for the removal of amido black 10B, J. Chem. Eng. Data 55 (2010) 3489–3493.
[15] R. Ahmad, R. Kumar, Adsorptive removal of congo red dye from aqueous solution using bael shell carbon, Appl. Surf. Sci. 257 (2010) 1628–1633.
[16] H. Daraei, A. Mittal, J. Mittal, H. Kamali, Optimization of Cr(VI) removal onto biosorbent eggshell membrane: Experimental & theoretical approaches, Desalin. Water Treat. 52 (2014) 1307–1315.
[17] J. Mittal, D. Jhare, H. Vardhan, A. Mittal, Utilization of bottom ash as a low-cost sorbent for the removal and recovery of a toxic halogen containing dye eosin yellow, Desalin. Water Treat. 52 (2014) 4508–4519.
[18] H. Demir, A. Top, D. Balköse, S. Ülkü, Dye adsorption behavior of *Luffa cylindrica* fibers, J. Hazard. Mater. 153 (2008) 389–394.
[19] J.X. Yu, L.Y. Wang, R.A. Chi, Y.F. Zhang, Z.G. Xu, J. Guo, Removal of cationic dyes: Basic magenta and methylene blue from aqueous solution by adsorption on modified loofah, Res. Chem. Intermed. 39 (2013) 3775–3790.

[20] N.A. Oladoja, C.O. Aboluwoye, A.O. Akinkugbe, Evaluation of loofah as a sorbent in the decolorization of basic dye contaminated aqueous system, Ind. Eng. Chem. Res. 48 (2009) 2786–2794.
[21] D.V. Kosynkin, D.C. Marcano, J.M. Berlin, A. Sinitskii, Z. Sun, A. Slesarev, L.B. Alemany, W. Lu, J.M. Tour, Improved synthesis of graphene oxide, ACS Nano 4 (2010) 4806–4814.
[22] P. Sharma, N. Hussain, D.J. Borah, M.R. Das, Kinetics and adsorption behavior of the methyl blue at the graphene oxide/reduced graphene oxide nanosheet–water interface: A comparative study, J. Chem. Eng. Data 58 (2013) 3477–3488.
[23] T. Liu, Y. Li, Q. Du, J. Sun, Y. Jiao, G. Yang, Z. Wang, Y. Xia, W. Zhang, K. Wang, H. Zhu, D. Wu, Adsorption of methylene blue from aqueous solution by graphene, Colloids Surf., B: Biointerfaces 90 (2012) 197–203.
[24] N. Pan, J.G. Deng, D.B. Guan, Y.D. Jin, C.Q. Xia, Ultralow temperature synthesis and improved adsorption performance of graphene oxide nanosheets, Appl. Surf. Sci. 324 (2015) 363–368.
[25] N. Pan, J.G. Deng, D.B. Guan, Y.D. Jin, C.Q. Xia, Adsorption characteristics of Th(IV) ions on reduced graphene oxide from aqueous solutions, Appl. Surf. Sci. 287 (2013) 478–483.
[26] M. Hasanzadeh, N. Shadjou, (Fe_3O_4)-graphene oxide-SO_3H as a new magnetic nanocatalyst for electro-oxidation and determination of selected parabens, J. Nanosci. Nanotechnol. 13 (2013) 4909–4916.
[27] L. Fan, C. Luo, M. Sun, H. Qiu, X. Li, Synthesis of magnetic β-cyclodextrin–chitosan/graphene oxide as nanoadsorbent and its application in dye adsorption and removal, Colloids Surf., B: Biointerfaces 103 (2013) 601–607.
[28] L. Li, L. Fan, M. Sun, H. Qiu, X. Li, H. Duan, C. Luo, Adsorbent for hydroquinone removal based on graphene oxide functionalized with magnetic cyclodextrin-chitosan, Int. J. Biol. Macromol. 58 (2013) 169–175.
[29] L.L. Liu, J. Yu, X. Chen, Enhanced stability and reusability of alcohol dehydrogenase covalently immobilized on magnetic graphene oxide nanocomposites, J. Nanosci. Nanotechnol. 15 (2015) 1213–1220.
[30] Y.H. Ao, P.F. Wang, C. Wang, J. Hou, J. Qian, Preparation of grapheneoxide-Ag_3PO_4 composite photocatalyst with high visible light photocatalytic activity, Appl. Surf. Sci. 271 (2013) 265–270.
[31] D.X. Wang, L.L. Liu, X.Y. Jiang, J.G. Yu, X.H. Chen, X.Q. Chen, Adsorbent for p-phenylenediamine adsorption and removal based ongraphene oxide functionalized with magnetic cyclodextrin, Appl. Surf. Sci. 329 (2015) 197–205.
[32] N.A. Travlou, G.Z. Kyzas, N.K. Lazaridis, E.A. Deliyanni, Functionalization of graphite oxide with magnetic chitosan for the preparation of a nanocomposite dye adsorbent, Langmuir 29 (2013) 1657–1668.
[33] W.S. Hummers, R.E. Offeman, Preparation of graphitic oxide, J. Am. Chem. Soc. 80 (1958) 1339.
[34] S. Li, H. Huang, M. Tao, X. Liu, T. Cheng, Frontal polymerization preparation of poly(acrylamide-co-acrylic acid)/activated carbon composite hydrogels for dye removal, J. Appl. Polym. Sci. 129 (2013) 3737–3745.
[35] S. Li, H. Zhang, J. Feng, R. Xu, X. Liu, Facile preparation of poly(acrylic acid–acrylamide) hydrogels by frontal polymerization and their use in removal of cationic dyes from aqueous solution, Desalination 280 (2011) 95–102.
[36] S. Li, X. Liu, W. Huang, W. Li, X. Xia, S. Yan, J. Yu, Magnetically assisted removal and separation of cationic dyes from aqueous solution by magnetic nanocomposite hydrogels, Polym. Adv. Technol. 22 (2011) 2439–2447.
[37] B. Li, H. Cao, G. Yin, $Mg(OH)_2$@reduced graphene oxide composite for removal of dyes from water, J. Mater. Chem. 21 (2011) 13765–13768.
[38] X. Song, L. Lin, M. Rong, Y. Wang, Z. Xie, X. Chen, Mussel-inspired, ultralight, multifunctional 3D nitrogen-doped graphene aerogel, Carbon 80 (2014) 174–182.
[39] M.Z. Iqbal, A.A. Abdala, Thermally reduced graphene: synthesis, characterization and dye removal applications, RSC Adv. 3 (2013) 24455–24464.
[40] C. Chen, R. Li, L. Xu, D. Yan, Three-dimensional superhydrophobic porous hybrid monoliths for effective removal of oil droplets from the surface of water, RSC Adv. 4 (2014) 17393–17400.
[41] X. Tang, Q. Zhang, Z. Liu, K. Pan, Y. Dong, Y. Li, Removal of Cu(II) by loofah fibers as a natural and low-cost adsorbent from aqueous solutions, J. Mol. Liq. 191 (2014) 73–78.
[42] V.K. Gupta, S. Agarwal, P. Singh, D. Pathania, Acrylic acid grafted cellulosic Luffa cylindrical fiber for the removal of dye and metal ions, Carbohydr. Polym. 98 (2013) 1214–1221.
[43] A. Altınışık, E. Gür, Y. Seki, A natural sorbent, *Luffa cylindrica* for the removal of a model basic dye, J. Hazard. Mater. 179 (2010) 658–664.
[44] J.N. Tiwari, K. Mahesh, N.H. Le, K.C. Kemp, R. Timilsina, R.N. Tiwari, K.S. Kim, Reduced graphene oxide-based hydrogels for the efficient capture of dye pollutants from aqueous solutions, Carbon 56 (2013) 173–182.
[45] L. Sun, H. Yu, B. Fugetsu, Graphene oxide adsorption enhanced by *in situ* reduction with sodium hydrosulfite to remove acridine orange from aqueous solution, J. Hazard. Mater. 203–204 (2012) 101–110.
[46] F. Liu, S. Chung, G. Oh, T.S. Seo, Three-dimensional graphene oxide nanostructure for fast and efficient water-soluble dye removal, ACS Appl. Mater. Interfaces 4 (2012) 922–927.
[47] S. Chowdhury, P. Saha, Sea shell powder as a new adsorbent to remove Basic Green 4 (Malachite Green) from aqueous solutions: Equilibrium, kinetic and thermodynamic studies, Chem. Eng. J. 164 (2010) 168–177.
[48] S. Lagergren, About the theory of so-called adsorption of soluble substances, K. Sven. Vetenskapsakad. Handl. 24(4) (1898) 1–39.
[49] Y.S. Ho, G. McKay, Sorption of dye from aqueous solution by peat, Chem. Eng. J. 70 (1978) 115–124.
[50] I. Langmuir, The adsorption of gases on plane surfaces of glass, mica and platinum, J. Am. Chem. Soc. 40 (1918) 1361–1403.
[51] K.G. Bhattacharyya, A. Sarma, Adsorption characteristics of the dye, Brilliant Green, on Neem leaf powder, Dyes Pigm. 57 (2003) 211–222.
[52] H.M.F. Freundlich, Over the adsorption in solution, J. Phys. Chem. 57 (1906) 385–470.